ELSEVIER

Ceramics International 30 (2004) 2163–2169

CERAMICS INTERNATIONAL

www.elsevier.com/locate/ceramint

Aerosol deposition of dense lead zirconate titanate thin films at room temperature

Ming-Ren Huang [a], Cheng-Jien Peng [b], Hong-Yang Lu [a,*]

[a] *Institute of Materials Science and Engineering, National Sun Yat-Sen University, Kaohsiung 80424, Taiwan*
[b] *Materials Research Laboratories, Industrial Technology Research Institute, Chutung, Hsinchu 31015, Taiwan*

Received 9 September 2003; received in revised form 5 November 2003; accepted 10 December 2003
Available online 19 March 2004

Abstract

Lead zirconate titanate ($Pb(Zr,Ti)O_3$, PZT) films were grown on silicon ⟨1 0 0⟩ substrate by aerosol deposition, using solid-state reacted powder containing donor oxide Nb_2O_5, while the substrate was maintained at room temperature. The PZT films were simultaneously sintered upon deposition on a highly densified ceramic layer. Crystalline phases of the deposited films have been determined by X-ray diffractometry (XRD), and microstructures analysed by transmission electron microscopy (TEM). The cross-section microstructure consisted of several thin layers, including the PZT film and the platinum electrode and titanium-buffered layers on the substrate. High-resolution images revealed that the PZT layer contained a mixture of randomly oriented grains of nanometre size, which were embedded in an amorphous matrix. In contrast to the conventional liquid-phase sintering mechanism, sintering of the PZT films involved amorphised phases generated by pressure-induced amorphisation (PIA) from plastic deformation when the initial powder particles collided amongst one another upon reaching the silicon substrate during aerosol deposition. An analogy may be drawn to the impact of extraterrestrial meteorites in which diaplectic glass, i.e., amorphised phase, was formed and retained metastably at room temperature. The individual PZT grains were joined with the amorphised phase(s) and sintered to become a dense, thin film on the silicon substrate.

Keywords: A. Sintering; B. Electron microscopy; D. Perovskites; Electroceramics; Thin films

1. Introduction

A variety of piezoelectric thin film ferroelectrics, exhibiting promising piezoelectric properties, have been developed for the applications in non-volatile ferroelectric and dynamic memory (NvFRAM and DRAM) [1], and as sensors or actuators in the microelectromechanical systems (MEMS) [2,3]. Most of the PZT thin films for RAM and MEMS devices have been prepared [3] by chemical techniques via sol–gel [4,5] or metallorganic decomposition (MOD) routes [6]. Stable solution of the composition $Pb(Zr_{0.52}Ti_{0.48})O_3$ having lower coercivities near the morphotropic phase boundary (MPB), added with donor oxides such as Nb_2O_5 [7] to improve its ferroelectric properties, was spin-coated on platinum- and titanium-buffered silicon substrates [2,5,8–10]. Highly oriented PZT films of (1 1 1) and (1 0 0) texture [11], thought to be suitable for specific applications [1], have frequently been prepared by these techniques.

Concurrent to the crystallization of gels, the sol–gel films were usually fully densified in less than 60 s [8]. Most research on such films have therefore concentrated on how the preferred crystallographic orientations were evolved [12–15] in such a short time upon rapid thermal annealing (RTA) [16] at 400–700 °C [1–3,5,8,9] where useful ferroelectric properties were developed. Correlation between the physical properties and microstructure characteristics of the films was thus established. However, no emphasis has been made on the sintering of such films.

A modified sol–gel processing of PZT films was reported [17] to lower the sintering temperature to 450–650 °C. Liquid-phase additives, often of eutectic liquid compositions, have been adopted [18–21] to reduce the sintering temperature for bulk as well as thick-film type of PZT ceramics while retaining the piezoelectric properties. The successful additives, usually in the form of oxides, are ubiquitous [21]. For hard PZT, the sintering temperature

* Corresponding author. Tel.: +883-7-5254052; fax: +883-7-5256030.
E-mail address: hyl@mail.nsysu.edu.tw (H.-Y. Lu).

0272-8842/$30.00 © 2004 Elsevier Ltd and Techna S.r.l. All rights reserved.
doi:10.1016/j.ceramint.2003.12.003

has been decreased from 1250 to 1300 °C to just above 900 °C with MnO_2 [18], a mixture of PbF_2 and NaF [19]. Recently, PbO–Cu_2O mixture has enabled sintering of PZT with a composition near the MPB at 800 °C [20]. Adding the eutectic mixture of PbO–WO_3 [21], although resulting in a mechanically weaker ceramic, has reduced the sintering temperature of a hard PZT (with relative permittivity $\varepsilon_r > 1000$) from 1260 °C by ~200 °C.

An aerosol deposition technique, using ceramic powder, is being developed for the preparation of PZT thin films of high dielectric constant. The films are sintered to high densities upon deposition without the requirement of further annealing. The microstructural features were characteristic of the solid-state amorphisation [22] induced by high impact pressure [23,24] resembling extraterrestrial meteorite collision. A sintering mechanism involving the amorphised phases produced from plastic deformation upon impact of powder particles on the substrate and collision amongst them is proposed to account for the densification in aerosol-deposited PZT films at room temperature.

2. Experimental procedure

The initial PZT powder of $(Pb_{0.95}Sr_{0.05})((Zr_{0.52}Ti_{0.48})_{0.98}Nb_{0.02})O_3$ was prepared by solid-state reaction when 65.1 wt.% PbO, 20.1 wt.% ZrO_2, 11.7 wt.% TiO_2 added with 2.3 wt.% $SrCO_3$ and 0.8 wt.% Nb_2O_5 were mixed and calcined at 900 °C for 2 h. No excess PbO was used and the Zr/Ti ratio was kept at 0.52:0.48 near the MPB. The as-prepared PZT powder is expected to contain a slight deficiency of PbO from the initial powder mixture due to evaporation at 900 °C, but whose composition was not determined chemically. Crystalline phases were identified by XRD using a Siemens D5000 diffractometer (Karshrule, Germany) with Cu Kα radiation operating at 40 kV/30 mA and using Ni filter. The powder dispersed in ethanol was ultrasonicated before collected on a carbon-coated grid for examination under TEM.

Thin films were deposited on Pt- and Ti-buffered Si ⟨1 0 0⟩ substrates (i.e., Pt/Ti/SiO_2/Si) at room temperature. An aerosol was formed by introducing a carrier gas of Ar/O_2 mixture into a glass jar containing PZT powder, which was constantly agitated and maintained at ~5.3×10^4 Pa (400 Torr). It was then passed through a nozzle before reaching the substrate in a vacuum placed approximately 5 cm below the orifice to form PZT films. Each deposition has lasted for 20 min.

Crystalline phases in the as-deposited PZT samples were again determined via XRD. The as-deposited samples were then cut and stacked in epoxy resin before sliced and polished down to ~200 μm thick. One of them, unsliced, was polished and lapped down to 1 μm surface roughness using diamond paste and was observed under the SEM using a JEOL 6400 (Tokyo, Japan) after chemically etched in 30% HCl solution. Mounted on a glass slide, the stack of thin cross-sections was mechanically polished using diamond-embedded papers successively from #1000 to #8000. Samples were reduced to <20 μm thick before a copper grid was glued on using G1 glue (Gatan, Inc., Pleasanton, CA). Thin section was then cut along the circumference to discs of 3 mm (ϕ) with a scalpal. They were ion-beam thinned to electron transparency using a Gatan ion-miller (Duomill™). The cross-section microstructure was analysed via TEM using a JEOL AEM3010 operating at 300 kV. High resolution images have been processed with Digital Micrograph® software (Gatan, Inc.) to enhance contrast.

3. Results

3.1. Initial powders

Fig. 1 shows the crystalline reflections (trace (a)) conformed to PZT perovskite (JCPDS 33-784). The splitted reflections of $\{h\,k\,l\}$, however, suggest that the initial powder was orthorhombic, rather than tetragonal (*P4mmm* (No. 123)) [8]. Peak splitting into triplet reflections can be differentiated from the $\{2\,0\,0\}$ family at $2\theta \approx 44°$, by slow scanning at $0.01°\,s^{-1}$ for 10 s, and that is shown juxtaposed in Fig. 1. The lattice parameters of $a = 0.4022$ nm, $b = 0.4078$ nm and $c = 0.4104$ nm, where $a \neq b \neq c$, were determined by adopting the Nelson–Riley technique [25] when *four* families of reflections from trace (a) was used. The PZT phase has an expanded *b*-axis, comparing with

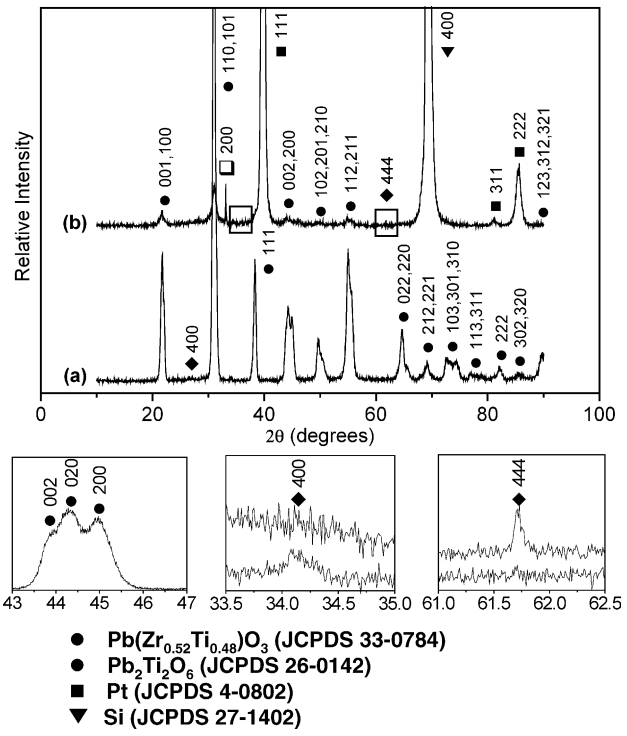

Fig. 1. XRD traces of (a) the initial powder, and (b) PZT films by aerosol deposition at room temperature.

data from JCPDS ($a = 0.4036$ nm and $c = 0.4146$ nm). The pseudo-tetragonal (orthorhombic) distortion of the c/a ratio ~1.02 lies near the composition of $Pb(Zr_{0.52}Ti_{0.48})O_3$ corresponding to MPB [26].

It also contained a trace amount of pyrochlore ($Pb_2(Zr,Ti)O_6$, JCPDS 26-0142, $Fd\bar{3}m$ (No. 227)), as suggested by $(4\,0\,0)_{py}$ reflections at $2\theta = 34.33^\circ$ shown in Fig. 1. Pyrochlore particles resulted from chemical imhomogeneity of the solid-state reacted powder can easily be identified from electron diffraction [27].

3.2. As-deposited films

Crystalline phases from the films deposited at room temperature are shown by XRD trace (b) in Fig. 1. Apart from PZT (reflections assigned according to JCPDS 33-0784), pyrochlore (py) has persisted in the deposited films as evidenced by $(4\,4\,4)_{py}$ at $2\theta = 61.75^\circ$. The $(1\,1\,1)_{PZT}$ reflection at $2\theta = 38.25^\circ$, clearly discernible from the initial powder in trace (a), was overwhelmed by $(1\,1\,1)_{Pt}$ of the textured Pt layer at $2\theta = 39.76^\circ$. The forbidden reflection of $(2\,0\,0)_{Si}$ at $2\theta = 32.98^\circ$ was originated from the multiple diffraction of the (1 0 0) single crystal silicon substrate [28].

Fig. 2a shows the cross-section view of the as-deposited films on Si substrate (i.e., layer (1)), which contained the barely resolved amorphous silica (SiO_2) layer and the Ti layer (appearing as a bright fringe indicated by arrow), and the Pt layer (2) of ~200–300 nm thick. On top of that is the epoxy resin (as indicated), which has survived ion-beam thinning. The PZT layer also of ~200–300 nm thick can be

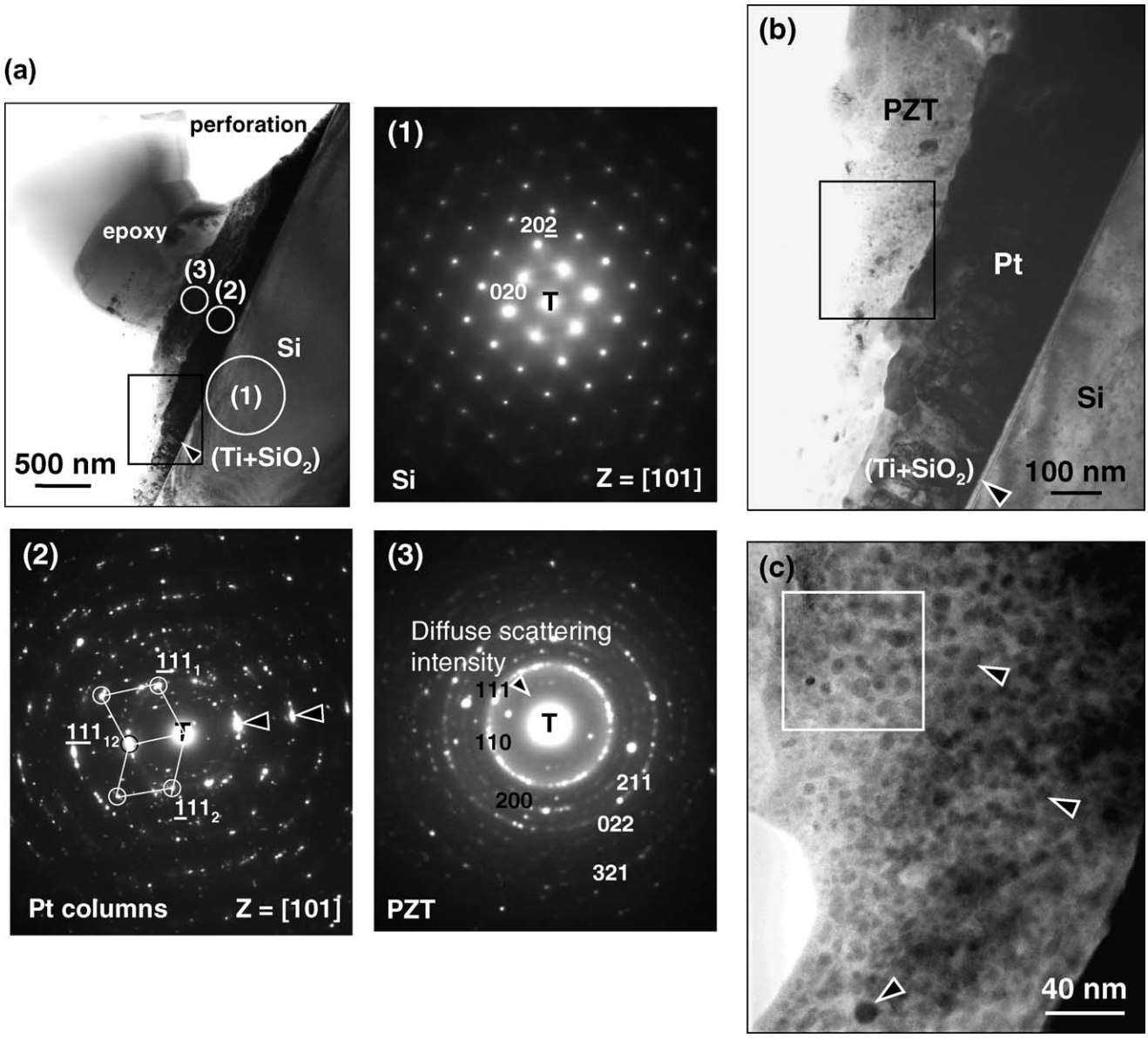

Fig. 2. Cross-section view of the as-deposited films containing Si substrate (layer (1)), Pt buffer layer (layer (2)), and randomly oriented PZT (layer (3)): (a) BF image with the corresponding SADPs, and (b) higher magnification of the area indicated in (a), and (c) higher magnification of the area indicated in (b) where PZT nano-grains are clearly discerned (TEM).

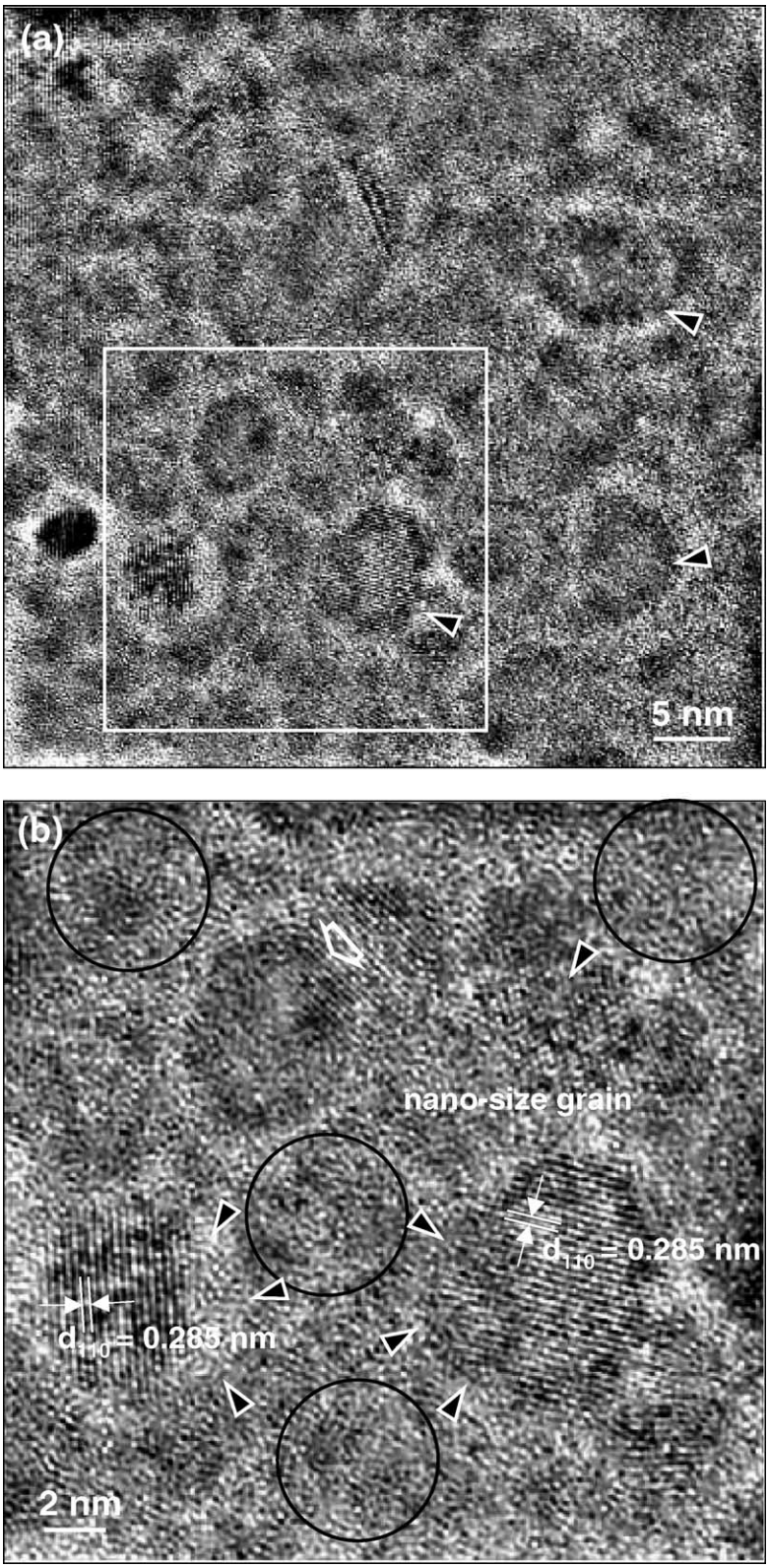

Fig. 3. (a) High-resolution images of the area indicated in Fig. 2b and c of the area indicated in (a) showing the matrix of highly disordered lattices, and coexistence of crystalline and amorphous phase in some of the grains (TEM).

unambiguously discerned (as indicated). The corresponding selected-area diffraction patterns (SADPs) for the three layers of (1) silicon, (2) Pt, and (3) PZT, that have been identified so far, are shown in juxtaposition. Twinning along $\langle 1\,1\,1\rangle_{Pt}$, as indicated, could also be determined where the twin spots from Pt grains are circled in pattern (2). The diffuse scattering intensity (DSI, as indicated in pattern (3)), most pronounced in the area circled by the $(1\,1\,0)_{PZT}$ ring, suggests that layer (3) contains phases of an amorphous nature. A higher magnification BF images, shown in Fig. 2b and c, revealed the randomly distributed, nano-size PZT grains between ~5 and 20 nm, as indicated by arrows, from the area indicated in Fig. 2a.

The ($Ti + SiO_2$)-layer appeared as two bright fringes [29] at higher magnification, as indicated in Fig. 2b. The PZT layer containing randomly dispersed polycrystalline grains of nanometre size between <5 and 40 nm, as suggested by the corresponding SADP of concentric rings (referred to Fig. 2a), is shown in Fig. 3a at a higher magnification. High resolution image in Fig. 3b revealed that the PZT grains were embedded in a matrix consisting of highly disordered [30], amorphous regions where well-defined lattice spacings cannot be determined. Both crystalline and amorphous phases co-existed in some of the PZT grains, one indicated by a blank arrow in Fig. 3b.

Almost all the nano-size grains examined have rounded corners characteristic to the liquid-phase sintered ceramics. The (1 1 0) lattice planes of PZT, with $d_{110} = 0.285$ nm (or $d_{101} = 0.289$ nm, but they were not differentiable) as indicated, can be determined from some of the PZT grains. In others, the crystal lattices constituting an aperiodic matrix were highly disordered both are indicated by blank arrows in Fig. 3b, and in which the crystal planes were barely visible. Further, many PZT grains have been undergoing amorphisation, as clearly evidenced from the collapsing lattices. The $(1\,1\,0)_{PZT}$ lattices (as indicated in Fig. 3b) in contiguity with an aperiodic region, immersing into the amorphous matrix, are distinguished unambiguously. Besides, the PZT grains of <10 nm are much smaller than the initial particles of submicron size (referred to Fig. 3a and b).

4. Discussion

The deposited films were dense ceramics where residual pores have rarely been detected (referred to Fig. 3a). The representative microstructure of PZT grains embedded in an amorphous matrix (referred to Fig. 3b), consisting of highly disordered lattices, indicates that the ceramic was densified by a liquid-phase sintering (LPS) mechanism.

Conventionally, LPS describes the process where a powder compact is densified with the assistance of a liquid phase formed in situ at sintering temperatures [31]. The sintering temperature is usually the eutectic point of a binary, ternary, or quaternary compound, or the melting point of another phase that is produced with the appropriate choice of sintering additive(s). Such liquid forms in the neck region between powder particles to facilitate atom diffusion when the ceramic is densified via a mechanism often referred to as the solution-diffusion-precipitation (S-D-P). The additive or additives usually operating for sintering at temperatures higher than 1200 °C, are therefore specific to a ceramic system, e.g., MgO [32], or Y_2O_3 [33] added to Si_3N_4, and $CaO + SiO_2$ added to Al_2O_3 [34], for improving sintering, and often desired properties, e.g., Bi_2O_3 added to donor-doped ZnO varistors [35] are developed simultaneously. A siliceous glassy grain-boundary phase has been unambiguously identified [32–35] in Si_3N_4 and Al_2O_3 ceramics by lattice-fringe imaging technique. That consequently has confirmed densification in these ceramics by a LPS mechanism was facilitated by liquid phase(s) formed at sintering temperatures due to the existence of a trace amount of impurities.

Whether the PZT films had been sintered by a LPS mechanism, two questions remain to be answered: (a) how was the liquid phase formed in aerosol-deposited thin films, and (b) did the liquid serve the same purpose as in the conventional sense that LPS has occurred at room temperature in aerosol-deposited thin films?

4.1. Amorphisation

Amorphisation of crystals is resulted from pressure variation [22–24] when a phase transformation occurs by PIA in the solid state. The geologists have long established [36,37] that diaplectic glass [38] of minerals such as quartz and feldspar in meteorite craters, showing no sign of flow, was formed at relatively low temperatures, far below its melting point, as a solid–solid phase transition by shock-wave compression (or decompression) from extraterrestrial meteorite collision [24,37]. In contrast, normal glass is produced by quenching from melts. Such PIA occurred by static compression–decompression, and shock waves has long been recognised [23,24] in minerals as well as in metallic alloys [39].

Perovskite $CaSiO_3$ stable at ~16 GPa was found [40] to transform into a mixture of glass and very small crystallites assigned to ε-$CaTiO_3$ [41] after release of pressure, i.e., decompression. Here, similarly, we have observed the decompressed perovskite PZT grains experienced the crystalline/amorphous phase transformation when the initial powder particles colliding amongst one another were compressed–decompressed, and instantaneously brought to a complete halt by the substrate during aerosol deposition. Some of the grains containing both phases, as indicated in Fig. 3b, were undergoing solid-state phase transformation upon collision at room temperature. In geological parlance, the amorphous phase is then better described as diaplectic glass of composition close to PZT, the initial powder composition. The experimental evidence showing rounded PZT grains dispersed in an aperiodic matrix strongly suggests that PIA occurs via shock-loading-like collision amongst

the initial PZT particles in the aerosol, and between the PZT particles and the substrate which was progressively built up with the incoming ceramic powder. PIA, a direct result of plastic deformation of PZT particles upon collision, has consequently produced the "liquid" phase which, having been amorphised, facilitated the sintering of PZT particles to become dense thin films (as seen from Fig. 2a).

4.2. Plastic deformation and liquid-phase sintering

The grains in thin films characterised by rounded corners [42,43], therefore, indicates that "dissolution" of PZT into a "liquid" phase has taken place at room temperature, i.e., the matrix exhibiting disordered lattices in Fig. 3a and b is an amorphised phase, or amorphised phases, by PIA due to plastic deformation upon impact. However, the PZT powder particles do not actually dissolve, nor does the dissolution occur in a "normal" liquid that is generated at above its eutectic or melting point [17–21]. In fact, dissolution may be seen as happened via amorphisation induced by mutual impact amongst powder particles when they are deformed plastically and altered to rounded shape concurrently (referred to Fig. 3a and b) on reaching the substrate.

Therefore, LPS in the conventional sense may be modified to describe a sintering mechanism where the "liquid-phase" is formed by solid-state amorphisation, which is sometimes termed "pseudo-melting" or "thermodynamic melting" [23], rather than by eutectic reaction or indeed melting of additive(s). It is unique that sintering of the PZT films although taking place in the presence of liquid phase(s), of an amorphous nature, does not rely on the conventional solution, diffusion, and so nor precipitation to achieve full densification, but on the plastically deformed particles that have become amorphous. The PZT films were sintered when the powder particles were plastically deformed and their surface or the whole particles amorphised in the solid-state. Therefore, densification has occurred by the assistance of the amorphous phase(s) produced through the random collisions amongst PZT particles upon arriving at the substrate. The plastic-deformation-induced soild-state amorphisation via a process similar to shock loading is analogous to extraterrestrial meteorite collision [37,38] at the nanometre scale.

5. Conclusions

PZT thin films made by aerosol deposition were densified via a liquid-phase sintering mechanism at room temperature. Some powder particles or the surfaces of particles were amorphised due to plastic deformation from mutual collisions upon arriving at the silicon substrate. The amorphisation forming diaplectic glass of composition close to PZT was induced by shock-wave-like impact and that is analogous to extraterrestrial meteorite collisions. The plastically deformed PZT particles, upon collision amongst themselves and with the substrate during aerosol deposition, have produced dense thin films sintered by the assistance of the amorphous phase.

Acknowledgements

Funding by the National Science Council and Ministry of Economic Affairs of Taiwan through contracts NSC 90-1126-E-110-018 and A311XS3241, respectively, is gratefully acknowledged.

References

[1] K. Aoki, Y. Fukuda, K. Numuta, A. Nishimura, Jpn. J. Appl. Phys. 33 (1994) 5155.
[2] H.D. Chen, K.R. Udayakumar, C.J. Gaskey, L.E. Cross, J. Am. Ceram. Soc. 79 (1996) 2189.
[3] B. Xu, L.E. Cross, J.J. Bernstein, Thin Solid Films 377/378 (2000) 712.
[4] K.D. Budd, S.K. Dev, D.A. Payne, Br. Ceram. Proc. 36 (1985) 107.
[5] B.A. Tuttle, J.A. Voigt, D.C. Goodnow, D.L. Lamppa, M.O. Eatough, G. Zender, R.D. Nasby, S.M. Rodgers, J. Am. Ceram. Soc. 76 (1993) 1537.
[6] J. Fukushima, K. Kodaira, T. Matsushima, J. Mater. Sci. 19 (1984) 595.
[7] A.H. Carim, B.A. Tuttle, D.H. Doughty, S.L. Martinez, J. Am. Ceram. Soc. 74 (1991) 1455.
[8] I.M. Reaney, K.G. Brooks, R. Klissurska, C. Pawlaczyk, N. Setter, J. Am. Ceram. Soc. 77 (1994) 1209.
[9] S.Y. Chen, I.W. Chen, J. Am. Ceram. Soc. 77 (1994) 2332.
[10] S.Y. Chen, I.W. Chen, J. Am. Ceram. Soc. 77 (1994) 2337.
[11] Y. Liu, P.P. Phule, J. Am. Ceram. Soc. 79 (1996) 495.
[12] C.K. Kwok, S.B. Desu, Appl. Phys. Lett. 60 (1992) 1430.
[13] A.P. Wilkinson, J.S. Speck, A.K. Cheetham, S. Natarajan, J.M. Thomas, Chem. Mater. 6 (1994) 750.
[14] J.A. Voigt, B.A. Tuttle, T.J. Headley, D.L. Lamppa, Mater. Res. Soc. Symp. Proc. 361 (1995) 395.
[15] A.D. Polli, F.F. Lange, C.G. Levi, J. Am. Ceram. Soc. 83 (2000) 873.
[16] J. Chen, K.R. Udayakumar, K.G. Brooks, L.E. Cross, J. Appl. Phys. 71 (1992) 4465.
[17] D.A. Barrow, T.E. Petroff, R.P. Tandon, M. Sayer, J. Appl. Phys. 81 (1997) 876.
[18] S.Y. Cheng, S.L. Fu, C.C. Wei, Ceram. Int. 13 (1987) 223.
[19] S. Takahashi, Jpn. J. Appl. Phys. 19 (1980) 771.
[20] D.L. Corker, R.W. Whatmore, E. Ringgaard, W.W. Wolny, J. Eur. Ceram. Soc. 20 (2000) 2039.
[21] E.R. Nielsen, E. Ringgaard, M. Kosec, J. Eur. Ceram. Soc. 22 (2002) 1847.
[22] W.L. Johnson, Prog. Mater. Sci. 30 (1986) 81.
[23] P. Richet, P. Gillet, Eur. J. Miner. 9 (1997) 907.
[24] S.M. Sharma, S.K. Sikka, Prog. Mater. Sci. 40 (2000) 1.
[25] B.D. Cullity, Elements of X-ray Diffraction, 2nd ed., Addison-Wesley, Reading, MA, 1976.
[26] B. Jaffee, W.R. Cook, H. Jaffee, Piezoelectric Ceramics, Academic Press, NY, 1971.
[27] M.R. Huang, C.J. Peng, H.Y. Lu, J. Am. Ceram. Soc. 86 (12) (2003) 2167–2175.
[28] B.H. Hwang, J. Phys. D: Appl. Phys. 34 (2001) 2469.
[29] D.R. Clarke, J. Am. Ceram. Soc. 63 (1980) 140.
[30] T.R. Welberry, A.G. Christy, J. Solid State Chem. 117 (1995) 323.
[31] R.J. Brook, Sci. Ceram. 9 (1977) 57.
[32] D.R. Clarke, G. Thomas, J. Am. Ceram. Soc. 60 (1977) 491.

[33] L.K.V. Lou, T.E. Mitchell, A.H. Heuer, J. Am. Ceram. Soc. 61 (1978) 392.
[34] M.P. Mallamaci, C.B. Carter, Acta Mater. 46 (1998) 2895.
[35] D.R. Clarke, J. Am. Ceram. Soc. 82 (1999) 485.
[36] P.S.D. Carli, J.C. Jamieson, J. Chem. Phys. 31 (1959) 1675.
[37] D.J. Milton, P.S.D. Carli, Science 140 (1963) 670.
[38] W.V. Engelhardt, J. Arndt, D. Stoffler, W.F. Muller, H. Jeziorkowski, R.A. Gubser, Contrib. Miner. Pertol. 15 (1976) 93.
[39] W.L. Johnson, Mater. Sci. Eng. 97 (1988) 1.
[40] L.G. Liu, A.E. Ringwood, Earth Planet. Sci. Lett. 28 (1975) 209.
[41] A.E. Ringwood, A. Major, Earth Planet. Sci. Lett. 12 (1971) 411.
[42] Y.M. Chiang, L.E. Silveman, R.H. French, R.M. Cannon, J. Am. Ceram. Soc. 77 (1994) 1143.
[43] C.J. Ting, C.S. Hsi, H.Y. Lu, J. Am. Ceram. Soc. 83 (2000) 2945.